Model predictive control using LPV approach for trajectory tracking of quadrotor UAV with external disturbances

Brajesh Kumar Singh and Awadhesh Kumar
Department of Electrical Engineering, Madan Mohan Malaviya University of Technology, Gorakhpur, India

Abstract

Purpose – The rotorcraft technology is very interesting area since last few decades due to variety of applications. One of the rotorcrafts is the quadrotor unmanned aerial vehicle (QUAV), which contains four rotors mounted on an airframe with an onboard controller. The QUAV is a highly nonlinear system and underactuated. Its controller design is very challenging task, and the need of controller is to make it autonomous based on mission planning. The purpose of this study is to design a controller for quadrotor UAV for attitude stabilization and trajectory tracking problem in presence of external environmental disturbances such as wind gust.

Design/methodology/approach – To address this problem, the model predictive control has been designed for attitude control and feedback linearization control for the position control using the linear parameter varying (LPV) approach. The trajectory tracking problem has been addressed using the circular trajectory and helical trajectory.

Findings – The simulation results show the efficient performance with good trajectory tracking even in presence of external disturbances in both the scenarios considered, one for circular trajectory tracking and other for helical trajectory tracking.

Originality/value – The novelty of the work came from using the LPV approach in controller design, which increases the robustness of the controller in presence of external disturbances.

Keywords Quadrotor, UAV, Linear parameter varying, model predictive control (MPC), Trajectory tracking

Paper type Research paper

1. Introduction

The autonomous aerial vehicle has fascinated the researchers since last few decades because of wide civilian and other applications like surveillance, military, product delivery, agriculture, search and rescue, aerial photography, entertainment and sports. Meanwhile, the scope for multirotor drones has also been increasing nowadays. The quadrotor has become very popular due to its simple or less complex dynamics as compared to other aerial vehicles.

The advantages of the quadrotor unmanned aerial vehicle (UAV) are high reliability, individual decision-making ability, mission variety and cheapness. The major challenges in design implementation of quadrotor drones are in its structure design, flight control system design. Many other factors which increase the complexity in the implementation of flight control systems are mass imbalance, wind, instability of blade rotation, parameter uncertainty, frame vibration due to motor rotation.

Many control schemes have been applied for the quadrotor flight control as well as trajectory tracking problem. Various linear controllers have been applied to the quadrotor as reported in the literature such as proportional integral derivative controller (Bolandi *et al.*, 2013; Chehadeh and Boiko, 2019; Salih *et al.*, 2010) and linear quadratic regulator (LQR) controller (García *et al.*, 2016; Outeiro *et al.*, 2021; Santos *et al.*, 2016). The fractional order control law (Efe, 2011; Oliva-Palomo *et al.*, 2019; Sadigh, 2019) has been applied to QUAV to achieve good tracking and robustness. The nonlinear control techniques have also been applied for robust performance and better tracking ability of the controller such as feedback linearization control, backstepping controller and sliding mode control. The feedback linearization control (Freddi *et al.*, 2011; Lee *et al.*, 2009) aims to deal with nonlinear dynamics of the system while backstepping controller (Bouabdallah and Siegwart, 2005; Chen *et al.*, 2016; Liu *et al.*, 2019) usually works in presence of input saturation and external disturbances. The sliding mode control (Eltayeb *et al.*, 2020; Ghadiri *et al.*, 2021) is usually applied for enhancing disturbance rejection capability and avoids mismatched exogenous disturbance. The hybrid version of backstepping and sliding mode control has also been applied to quadrotor control (Jia *et al.*, 2017) to avoid chattering and increase robustness known as integral backstepping sliding mode control. The adaptive and robust control schemes are implemented for quadrotor control such as gain scheduling controller (Qiao *et al.*, 2018) for varying operating condition to increase fault tolerance capability, H_∞ control (Guo *et al.*, 2017; Prempain and Postlethwaite, 2005) in case of noisy measurement and environmental disturbances. Most of the above design techniques are having drawbacks in implementation like gain

The current issue and full text archive of this journal is available on Emerald Insight at: **https://www.emerald.com/insight/1748-8842.htm**

Aircraft Engineering and Aerospace Technology
 [ISSN 1748-8842]
[DOI 10.1108/AEAT-12-2021-0368]

Received 12 December 2021
Revised 20 May 2022
8 August 2022
Accepted 2 September 2022

switching in case of gain scheduling control, actuator fault, network delay and variable time communication structure. An extended state observer is also used in the control design for the quadrotor (Gai *et al.*, 2018) which was found to compensate the effect of wind disturbances efficiently. The model predictive control (MPC) is also widely used control technique now a days in aerospace applications, which have been reported in literature (Abdolhosseini *et al.*, 2013; Alexis *et al.*, 2012; Misin and Puig, 2020) for quadrotor control. The intelligent control schemes have also been designed and implemented in the literature such as neural network (Dierks and Jagannathan, 2010; Jiang *et al.*, 2020), fuzzy logic control (Sol *et al.*, 2021; Torres *et al.*, 2016), machine learning (Cen *et al.*, 2021; Nascimento *et al.*, 2020) and neuro fuzzy (Cervantes-Rojas *et al.*, 2020; Cervantes *et al.*, 2017). There are various advantages of artificial intelligence based controllers such as system identification ability when dynamic equations are difficult to derive, ability to handle model uncertainty and precise estimation of perturbations etc. Many more control schemes are also applied to quadrotor in hybrid mode where advantages of two or more control schemes are used over the disadvantages of the controllers.

In this paper, the MPC is used with feedback linearization control in cascade where the inner loop is controlled by the MPC, and for the outer loop, feedback linearization control has been used in presence of external atmospheric disturbances such as wind gust. The organization of the paper is described as follows: in Section 2, the problem statement has been briefly discussed which have been implemented in this paper. The dynamic modeling of the QUAV system has been derived using the first principles in the Section 3. In the Section 4, the proposed control design and the mathematical formulation have been presented. The simulation results have been discussed in Section 5 where the two different scenarios have been presented for two trajectories. The conclusion of the aforesaid research work is mentioned in Section 6.

2. Problem statement

The QUAV is an underactuated nonlinear system because it has fewer number of actuators than the degree of freedom (DoF) to be controlled, so its control design is very challenging task. The problem statement of QUAV control may be stated as:

- to design a controller for the attitude stabilization and trajectory tracking problem in presence of external atmospheric disturbances; and
- to overcome the design complexity, through linear parameter varying approach in discrete domain.

3. Mathematical modeling of quadrotor

In this section, the mathematical modeling of the system has been derived using the first principles of rigid body motion. The QUAV is an underactuated system having six-degrees of freedom. There are four rotors in the QUAV in which two opposite facing rotors rotate in clockwise and other two rotate in counterclockwise direction. The schematic diagram for a quadrotor with body and earth reference frame has been depicted in Figure 1.

The position and attitude vector of the quadcopter in earth frame are defined by $\xi^E = [x\ y\ z]^T$ and $\eta^E = [\phi\ \theta\ \psi]^T$ where ϕ is rotation about inertial x-axis called roll angle; θ is rotation about inertial y-axis is pitch angle; and ψ is rotation about

Figure 1 Schematic representation of a Quadrotor UAV

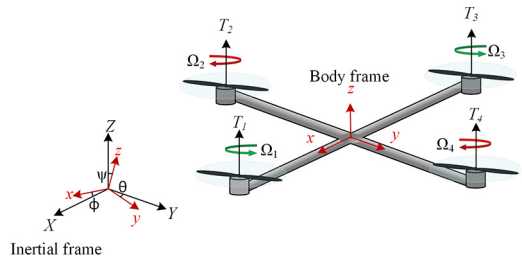

inertial z-axis and known as yaw angle. The translational and rotation velocities are defined in body frame $V^B = [u\ v\ w]^T$ and $\omega^B = [p\ q\ r]^T$. The rotation matrix R is used to convert body frame velocities into inertial frame positions derivative:

$$\dot{\xi}^E = RV^B \tag{1}$$

$$R = \begin{bmatrix} \cos\theta\cos\psi & \sin\phi\sin\theta\cos\psi - \cos\phi\sin\psi & \cos\phi\sin\theta\cos\psi + \sin\phi\sin\psi \\ \cos\theta\sin\psi & \sin\phi\sin\theta\sin\psi + \cos\phi\cos\psi & \cos\phi\sin\theta\sin\psi - \sin\phi\cos\psi \\ -\sin\theta & \sin\phi\cos\theta & \cos\phi\cos\theta \end{bmatrix} \tag{2}$$

The attitude in earth frame can be derived from body frame angular velocity by using transformation matrix T, which is obtained as:

$$\dot{\eta}^E = T\omega^B \tag{3}$$

$$T = \begin{bmatrix} 1 & \sin\phi\tan\theta & \cos\phi\tan\theta \\ 0 & \cos\phi & -\sin\phi \\ 0 & \dfrac{\sin\phi}{\cos\theta} & \dfrac{\cos\phi}{\cos\theta} \end{bmatrix} \tag{4}$$

The dynamics of the quadrotor is defined by 6-DoF Newton–Euler equations for forces and moments in the body frame. The translational dynamics of the quadrotor system has been defined by the following forces equation:

$$F^B = m\left(\dot{V}^B + \omega^B \times V^B\right) \tag{5}$$

where m is the total mass of the quadrotor and forces $F^B = [F_x\ F_y\ F_z]^T$. The rotational dynamics of the system has been defined by following moment equation:

$$M^B = I^B\dot{\omega}^B + \omega^B \times (I^B\omega^B) \tag{6}$$

Where I^B is the inertia matrix in body frame which is given in equation (5) and moments in body frame $M^B = [M_x\ M_y\ M_z]^T$ around body frame x-, y- and z-axes:

$$I^B = \begin{bmatrix} I_{xx} & 0 & 0 \\ 0 & I_{yy} & 0 \\ 0 & 0 & I_{zz} \end{bmatrix} \tag{7}$$

where I_{xx}, I_{yy} and I_{zz} are the inertia of the quadrotor around body frame x-, y- and z-axes. From equations (3) and (4) the following equation of rigid body motion is obtained:

$$M\dot{v}^B + C^B(v^B)v^B = \Lambda^B \tag{8}$$

where $v^B = [u\ v\ w\ p\ q\ r]^T$ is velocity vector; $C^B(v^B) \in \mathbb{R}^{6\times6}$ depends upon velocity vector; and $M \in \mathbb{R}^{6\times6}$ contains mass and moments, and $\Lambda^B = [F_x\ F_y\ F_z\ M_x\ M_y\ M_z]^T$ *is net force-moment vector contains force-moment due to gravity* Λ_g^B, gyroscopic effect Λ_{gr}^B and control input Λ_{in}^B which is described by equation (7):

$$\Lambda^B = \Lambda_g^B + \Lambda_{gr}^B + \Lambda_{in}^B \tag{9}$$

The state space for of quadrotor dynamics can be obtained as:

$$\dot{v}^B = M^{-1}[\Lambda^B - C^B(v^B)v^B] \tag{10}$$

The detailed state space equations of the quadrotor system have been described as below:

$$\left.\begin{aligned}
\dot{u} &= vr - wq + g\sin\theta \\
\dot{v} &= wp - ur - g\cos\theta\sin\phi \\
\dot{w} &= uq - vp - g\cos\theta\cos\phi + \frac{U_1}{m} \\
\dot{p} &= \left(\frac{I_{yy} - I_{zz}}{I_{xx}}\right)qr + \frac{\mathcal{J}_{tp}}{I_{xx}}q\Omega + \frac{U_2}{I_{xx}} \\
\dot{q} &= \left(\frac{I_{zz} - I_{xx}}{I_{yy}}\right)pr - \frac{\mathcal{J}_{tp}}{I_{yy}}p\Omega + \frac{U_3}{I_{yy}} \\
\dot{r} &= \left(\frac{I_{xx} - I_{yy}}{I_{zz}}\right)pq + \frac{U_4}{I_{zz}}
\end{aligned}\right\} \tag{11}$$

The angular speed of propeller Ω_i, where i = 1,2,3,4 for four rotors in which rotor 1 and 3 rotating counterclockwise and rotor 2 and 4 rotating clockwise and the net angular speed is Ω:

$$\Omega = \Omega_1 - \Omega_2 + \Omega_3 - \Omega_4 \tag{12}$$

The control input U_1 is the total thrust generated by the propellers in terms of angular speed of the propellers, and C_T is the thrust factor:

$$U_1 = \sum_{i=1}^{4} T_i = C_t \sum_{i=1}^{4} \Omega_i^2 \tag{13}$$

The moments of the quadrotor about the body frame x-, y- and z-axes are U_2, U_3 and U_4 which is obtained as:

$$\begin{bmatrix} U_2 \\ U_3 \\ U_4 \end{bmatrix} = \begin{bmatrix} C_t l(\Omega_2^2 - \Omega_4^2) \\ C_t l(\Omega_3^2 - \Omega_1^2) \\ C_q(-\Omega_1^2 + \Omega_2^2 - \Omega_3^2 + \Omega_4^2) \end{bmatrix} \tag{14}$$

where C_Q is the drag factor and l is the distance between center of mass and the propeller axis.

The physical parameters used in the above modeling and for simulation has been provided in the Table 1.

3.1 Modeling of disturbances

In the outdoor operation of the QUAV, the external atmospheric disturbances are always present such as wind gust, which affects the stability and tracking performance of the controller designed for quadrotor. The vectorial representation of the disturbances $\boldsymbol{d} = [\boldsymbol{d_1}\ \boldsymbol{d_2}]^T$ is modeled as given in below equations:

$$m\dot{V}^B = F^B - m(\omega^B \times V^B) + d_1 \tag{15}$$

$$I^B\dot{\omega}^B = M^B - \omega^B \times (I^B\omega^B) + d_2 \tag{16}$$

where $\boldsymbol{d_1}$ is modeled as force disturbance and $\boldsymbol{d_2}$ is modeled as moment disturbance. These disturbances are characterized by two parts: constant disturbance and stochastic disturbance:

$$\mathrm{d_i} = \mathrm{d_{ic}} + \mathrm{d_{is}}$$

where i = 1,2 and d_{ic} is the constant disturbances which are due to static wind and are slowly varying with time. d_{is} is the disturbance due to stochastic wind or fast varying disturbances. The stochastic disturbances are modeled by additive white Gaussian noise assuming 30 dB signal to noise ratio which is high intensity wind disturbance to the quadrotor system.

4. Trajectory tracking controller design

The quadrotor system has a smaller number of inputs than outputs of the system. The proposed control architecture has been applied in inner loop for attitude control and outer loop for position control. The schematic diagram for the proposed control architecture has been shown in the Figure 2.

For position control, the feedback linearization technique is used to design the controller for translational subsystem and MPC for attitude control for rotational subsystem. The coordination of both the controllers are very important to achieve the desired control objective. The iteration of inner loop is 4 times more, as compared to the outer loop iteration for efficient tracking performance of the MPC. Therefore, sampling period for inner loop has been adjusted to 0.1 s and that for outer loop has been adjusted to 0.4 s. Both the controllers are designed in discrete domain because the MPC requires discrete model of the system or plant.

4.1 Position controller

For the position control system, the translational equation of motion has been used in inertial frame of reference as obtained in equation (17):

$$\left.\begin{aligned}
\ddot{x} &= (\cos\phi\sin\theta\cos\psi + \sin\phi\sin\psi)\ U_1/m \\
\ddot{y} &= (\cos\phi\sin\theta\sin\psi - \sin\phi\cos\psi)\ U_1/m \\
\ddot{z} &= -g + \cos\phi\cos\theta U_1/m
\end{aligned}\right\} \tag{17}$$

The reference trajectory is generated by the trajectory planner and the reference value as x_{ref}, y_{ref} and z_{ref} and the actual value of the x, y and z from the plant. The errors for three positions are obtained as:

Table 1 Physical parameters of the QUAV

Symbol	Description	Value (unit)
m	Mass of QUAV	0.698 (Kg)
g	Acceleration due to gravity	9.81 (m/s^2)
I_{xx}	Moment of inertia along body frame x-axis	0.0034 (Kg/m^2)
I_{yy}	Moment of inertia along body frame y-axis	0.0034 (Kg/m^2)
I_{zz}	Moment of inertia along body frame z-axis	0.006 (Kg/m^2)
J_{tp}	Moment of inertia of motor along propeller axis	1.302×10^{-6}(Kg/m^2)
C_t	Thrust factor	3.948×10^{-7} (N-s^2)
C_q	Torque factor	4.078×10^{-9} (N-m-s^2)
l	Distance between center of mass and propeller axis	0.171 (m)

Figure 2 Control architecture with two feedback-loops for the Quadcopter UAV

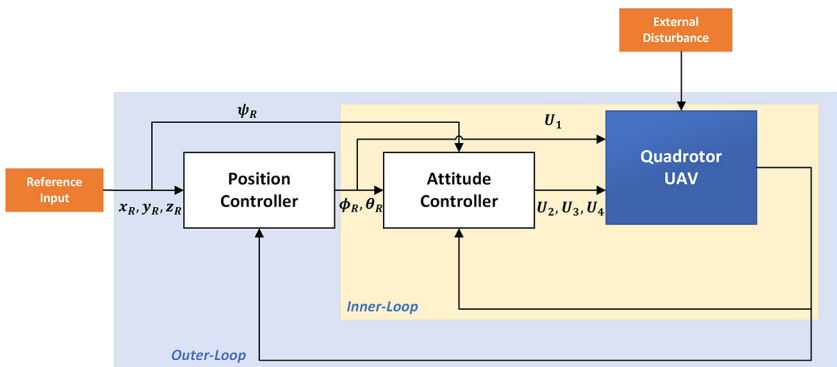

$$\left.\begin{aligned} e_x &= x_{ref} - x \\ e_y &= y_{ref} - y \\ e_z &= z_{ref} - z \end{aligned}\right\} \tag{18}$$

Now, the pole placement method is applied for the translational subsystem to make error, to converge it, to zero as time reaches infinite. The error differential equation for the pole placement controller is obtained as:

$$\ddot{e} = k_1 e + k_2 \dot{e} \tag{19}$$

The poles must be selected properly for the system, represented by error differential equation (19). Using pole placement technique for the desired pole, the state feedback gains have been obtained. These gains have been further used for finding the control law of the position controller for the three positions, which are the double derivatives of the three respective positions:

$$\begin{aligned} v_x &= k_{1x} e_x + k_{2x} \dot{e}_x \\ v_y &= k_{1y} e_y + k_{2y} \dot{e}_y \\ v_z &= k_{1z} e_z + k_{2z} \dot{e}_z \end{aligned} \tag{20}$$

The reference values for roll and pitch angles and the total thrust force are obtained by the control actions. The control action U1 and reference values of pitch and roll angles can be obtained from the following equations:

$$U_1 = \frac{m(\ddot{z} + g)}{\cos\phi \cos\theta} \tag{21}$$

$$\theta_{ref} = \tan^{-1}\left(\frac{\ddot{x}}{\ddot{z} + g}\cos\psi_{ref} + \frac{\ddot{y}}{\ddot{z} + g}\sin\psi_{ref}\right) \tag{22}$$

The reference value of roll angle depends on two conditions:

- *for* $0 < \psi_{ref} < \pi/4$ *or* $3\pi/4 < \psi_{ref} < 5\pi/4$ *or* $7\pi/4 < \psi_{ref} < 2\pi$

$$\phi_{ref} = \tan^{-1}\left[\frac{\cos\theta\left(\tan\theta\sin\psi_{ref} - \frac{\ddot{y}}{\ddot{z} + g}\right)}{\cos\psi_{ref}}\right] \tag{23}$$

- for conditions other than above, the value of roll angle is obtained:

$$\phi_{ref} = \tan^{-1}\left[\frac{\cos\theta\left(\frac{\ddot{x}}{\ddot{z} + g} - \tan\theta\cos\psi_{ref}\right)}{\cos\psi_{ref}}\right] \tag{24}$$

The reference angles for roll and pitch (ϕ_{ref} and θ_{ref}) are fed to the MPC controller and thrust force as the final control input U_1 is fed to the plant.

4.2 Attitude controller

The attitude controller is the inner-loop controller that is designed to stabilize the attitude of the QUAV. The rotational

equation of motion is used for designing MPC attitude controller with small angle approximation. It is assumed that the roll and pitch angles are small to ensure stable flight and good trajectory tracking of the vehicle. By taking above assumption, the following equations of rotational motion have been obtained:

$$\left.\begin{aligned}\ddot{\phi} &= \left(\frac{I_{yy}-I_{zz}}{I_{xx}}\right)\dot{\theta}\dot{\psi} + \frac{\mathcal{J}_{tp}}{I_{xx}}\dot{\theta}\,\Omega + U_2/I_{xx}\\ \ddot{\theta} &= \left(\frac{I_{zz}-I_{xx}}{I_{yy}}\right)\dot{\phi}\dot{\psi} + \frac{\mathcal{J}_{tp}}{I_{yy}}\dot{\phi}\,\Omega + U_3/I_{yy}\\ \ddot{\psi} &= \left(\frac{I_{xx}-I_{yy}}{I_{zz}}\right)\dot{\phi}\dot{\theta} + U_4/I_{zz}\end{aligned}\right\} \tag{25}$$

The above equations can be put in state-space form with system matrix dependent on states of the system. The horizon period (N_P) of the MPC controller is taken as 4; it means the MPC can predict the future states for four sample times. After putting the above nonlinear equations in state space, the matrices can be represented as equation (26):

$$\left.\begin{aligned}\dot{x} &= Ax + Bu\\ y &= Cx + Du\end{aligned}\right\} \tag{26}$$

where $x \in \mathbb{R}^6$ is the state vector; $u \in \mathbb{R}^3$ the input vector; and $y \in \mathbb{R}^3$ is output vector, and A, B, C and D matrices are obtained as given below:

$$A = \begin{bmatrix} 0 & 1 & 0 & 0 & 0 & 0\\ 0 & 0 & 0 & A_{24} & 0 & A_{26}\\ 0 & 0 & 0 & 1 & 0 & 0\\ 0 & A_{42} & 0 & 0 & 0 & A_{46}\\ 0 & 0 & 0 & 0 & 0 & 1\\ 0 & A_{62} & 0 & A_{64} & 0 & 0 \end{bmatrix}, \quad B = \begin{bmatrix} 0 & 0 & 0\\ 1/I_{xx} & 0 & 0\\ 0 & 0 & 0\\ 0 & 1/I_{yy} & 0\\ 0 & 0 & 0\\ 0 & 0 & 1/I_{zz} \end{bmatrix}$$

$$C = \begin{bmatrix} 1 & 0 & 0 & 0 & 0 & 0\\ 0 & 0 & 1 & 0 & 0 & 0\\ 0 & 0 & 0 & 0 & 1 & 0 \end{bmatrix}, \quad D = \begin{bmatrix} 0 & 0 & 0\\ 0 & 0 & 0\\ 0 & 0 & 0 \end{bmatrix}$$

$$A_{24} = \frac{\mathcal{J}_{tp}}{I_{xx}}\,\Omega, \quad A_{26} = \frac{I_{yy}-I_{zz}}{I_{xx}}\dot{\theta}, \quad A_{42} = -\frac{\mathcal{J}_{tp}}{I_{yy}}\,\Omega,$$

$$A_{46} = \frac{I_{zz}-I_{xx}}{I_{yy}}\dot{\phi}, \quad A_{62} = \frac{I_{xx}-I_{yy}}{I_{zz}}\frac{\dot{\theta}}{2}, \quad A_{64} = \frac{I_{xx}-I_{yy}}{I_{zz}}\frac{\dot{\phi}}{2}$$

The discretization of the above state-space equations has been done to obtain following discrete state-space equation (27):

$$\left.\begin{aligned}x_{k+1} &= A_d x_k + B_d u_k\\ y_k &= C_d x_k\end{aligned}\right\} \tag{27}$$

The future states are predicted by using the general solution of the above state equation, which is obtained as in equation (28):

$$x_k = A_d^k x_0 + \begin{bmatrix} A_d^{k-1}B_d & A_d^{k-2}B_d & \cdots & A_dB_d & B_d \end{bmatrix} \begin{bmatrix} u_0\\ u_1\\ \vdots\\ u_{k-2}\\ u_{k-1} \end{bmatrix} \tag{28}$$

The A_d matrix is different for each k = 1 *to* 4, but the matrix does not change as much, and the angular speed is also constant for a horizon period. So, for simplicity and to reduce computational burden, the same A_d matrix has been used.

4.2.1 Cost function minimization

The cost function for the system is a quadratic cost function in terms of errors and change in input to ensure the change in control input as small as possible for smooth control action. Therefore, the following augmented state-space equation is obtained:

$$\left.\begin{aligned}\begin{bmatrix} x_{k+1}\\ u_k \end{bmatrix} &= \begin{bmatrix} A_d & B_d\\ 0 & I \end{bmatrix}\begin{bmatrix} x_k\\ u_{k-1} \end{bmatrix} + \begin{bmatrix} B_d\\ I \end{bmatrix}\Delta u_k\\ y_k &= \begin{bmatrix} C_d & 0 \end{bmatrix}\begin{bmatrix} x_k\\ u_{k-1} \end{bmatrix}\end{aligned}\right\} \tag{29}$$

$$\left.\begin{aligned}\tilde{x}_{k+1} &= \tilde{A}_d\tilde{x}_k + \tilde{B}_d\Delta u_k\\ y_k &= \tilde{C}_d\tilde{x}_k\end{aligned}\right\} \tag{30}$$

The cost function has been obtained as given in equation (31):

$$\mathcal{J} = \frac{1}{2}e_{k+N}^T S e_{k+N} + \frac{1}{2}\sum_{i=0}^{N-1} e_{k+i}^T Q e_{k+i} + \Delta u_{k+i}^T R \Delta u_{k+i} \tag{31}$$

After some manipulation, the constant terms are removed from the cost function we obtain following cost function:

$$\mathcal{J}'' = \frac{1}{2}\tilde{x}_G^T\overline{\overline{Q}}\tilde{x}_G - \tilde{r}_G^T\overline{\overline{T}}\,\tilde{r}_G + \frac{1}{2}\Delta u_G^T\overline{\overline{R}}\Delta u_G \tag{32}$$

where $\tilde{x}_G$ is the global augmented state vector; Δu_G is the global augmented control vector; $\tilde{r}_G$ is the global augmented reference vector; and the weight matrices of above cost function are defined as:

$$\overline{\overline{Q}} = \begin{bmatrix} \tilde{C}^T Q\tilde{C} & 0_{9\times9} & 0_{9\times9} & 0_{9\times9}\\ 0_{9\times9} & \tilde{C}^T Q\tilde{C} & 0_{9\times9} & 0_{9\times9}\\ 0_{9\times9} & 0_{9\times9} & \tilde{C}^T Q\tilde{C} & 0_{9\times9}\\ 0_{9\times9} & 0_{9\times9} & 0_{9\times9} & \tilde{C}^T S\tilde{C} \end{bmatrix};$$

$$\overline{\overline{T}} = \begin{bmatrix} Q\tilde{C} & 0_{3\times9} & 0_{3\times9} & 0_{3\times9}\\ 0_{3\times9} & Q\tilde{C} & 0_{3\times9} & 0_{3\times9}\\ 0_{3\times9} & 0_{3\times9} & Q\tilde{C} & 0_{3\times9}\\ 0_{3\times9} & 0_{3\times9} & 0_{3\times9} & S\tilde{C} \end{bmatrix};$$

$$\overline{\overline{R}} = \begin{bmatrix} R & 0_{3\times3} & 0_{3\times3} & 0_{3\times3}\\ 0_{3\times3} & R & 0_{3\times3} & 0_{3\times3}\\ 0_{3\times3} & 0_{3\times3} & R & 0_{3\times3}\\ 0_{3\times3} & 0_{3\times3} & 0_{3\times3} & R \end{bmatrix}$$

The state vector for one horizon period is found using the below formula:

$$\begin{bmatrix} \widetilde{x}_{k+1} \\ \widetilde{x}_{k+2} \\ \widetilde{x}_{k+3} \\ \widetilde{x}_{k+4} \end{bmatrix} = \begin{bmatrix} \widetilde{B} & 0 & 0 & 0 \\ \widetilde{A}\widetilde{B} & \widetilde{B} & 0 & 0 \\ \widetilde{A}^2\widetilde{B} & \widetilde{A}\widetilde{B} & \widetilde{B} & 0 \\ \widetilde{A}^3\widetilde{B} & \widetilde{A}^2\widetilde{B} & \widetilde{A}\widetilde{B} & \widetilde{B} \end{bmatrix} \begin{bmatrix} \Delta u_k \\ \Delta u_{k+1} \\ \Delta u_{k+2} \\ \Delta u_{k+3} \end{bmatrix} + \begin{bmatrix} \widetilde{A} \\ \widetilde{A}^2 \\ \widetilde{A}^3 \\ \widetilde{A}^4 \end{bmatrix} \widetilde{x}_k \tag{33}$$

Above equation (33) can be simply represented as:

$$\widetilde{x}_G = \overline{\overline{C}}\Delta u_G + \hat{\widetilde{A}}\widetilde{x}_k$$

and the final simplified cost function has been obtained as in equation (34):

$$\mathcal{J} = \frac{1}{2}\Delta u_G^T H \Delta u_G + \begin{bmatrix} x_k^T & r_G^T \end{bmatrix} F^T \Delta u_G \tag{34}$$

$$H = \overline{\overline{C}}^T \overline{\overline{Q}}\,\overline{\overline{C}} + R, \quad F = \begin{bmatrix} \hat{\widetilde{A}}^T \overline{\overline{Q}}\,\overline{\overline{C}} & -\overline{\overline{T}}\,\overline{\overline{C}} \end{bmatrix}$$

The above cost function is minimized using quadratic programming method in MATLAB, and the optimized values of Δu_G are obtained, from which the optimized u_k is computed by using following relationship:

$$u_k = u_{k-1} + \Delta u_k \tag{35}$$

The MPC design parameters have been given in the Table 2.

The above design parameters are chosen to obtain less computational burden to the computer processors. The prediction horizon has been chosen to be four future predicted states for each controller sampling time, and control horizon is

Table 2 MPC controller design parameters

Parameter	Description	Value
N_P	Prediction horizon	4
N_C	Control horizon	4
Δt	Controller Sampling time	0.1 s
R	Weights on manipulated variable rates	$10I_{3\times3}$
Q	Weights on the output variables	$10I_{3\times3}$
S	Weights on final horizon outputs	$20I_{3\times3}$
[Ωmin, Ωmax]	Input constraints (motors rpm)	[1100, 8600]

Figure 3 Circular trajectory tracking plot for Quadrotor with and without the external disturbances

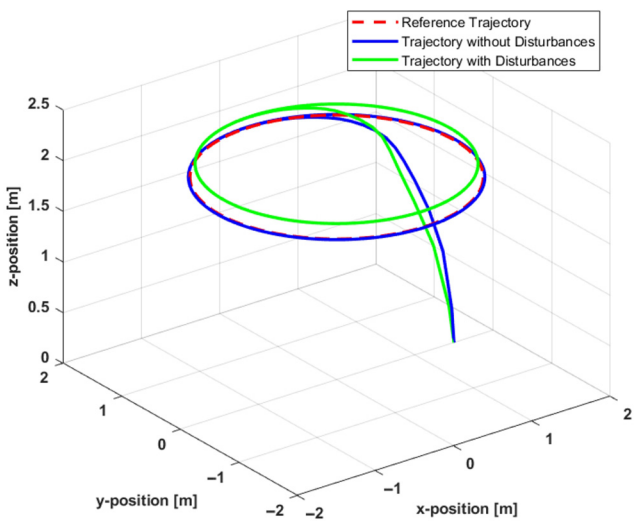

Figure 4 (a) Translational *x*-position, (b) *x*-velocity with and without external disturbances

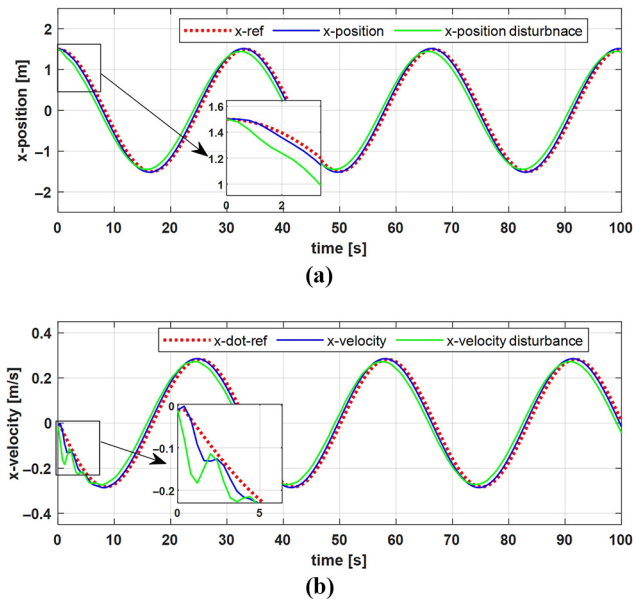

Figure 5 (a) Translational *y*-position, (b) *y*-velocity with and without external disturbances

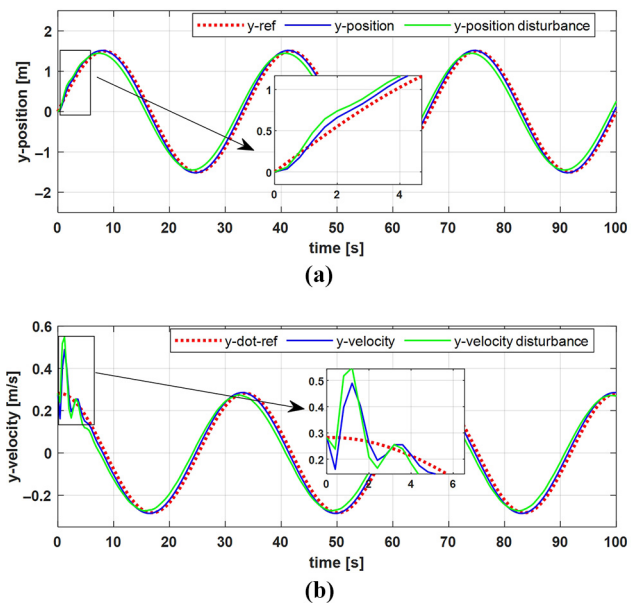

Figure 6 (a) Translational *z*-position, (b) *z*-velocity with and without external disturbances

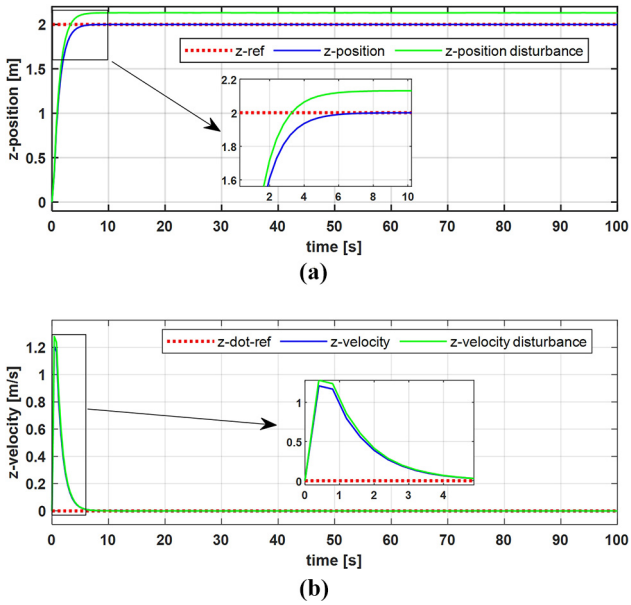

set to four to reduce the computing cost and get efficient performance of the controller. The input and output weights are chosen accordingly to obtain good controller response. The input constraints which are applicable to motor rpm speed are necessary to obtain real control action. So, these parameters are chosen to reduce the computational complexity and obtain efficient control action.

5. Results and discussion

The above-discussed control schemes have been simulated in MATLAB environment, considering the 6-DoF dynamic equations derived, which have been discussed in modeling section. The controller is tested for trajectory tracking with circular and helical trajectory in three-dimensional space. The trajectory tracking control of the controller without disturbances and in the presence of disturbances is presented through simulation results. Both the trajectory tracking cases are discussed in subsection 5.1 and 5.2, respectively.

5.1 Circular trajectory

The controller is first tested for a circular trajectory which is generated by the trajectory planner by providing the corresponding *x*, *y*, *z* positions in the earth reference frame and the reference yaw angle. The circular trajectory tracking for the quadrotor without disturbances and in presence of disturbances has been shown in Figure 3. It clearly shows the good trajectory tracking and excellent performance and robustness of the controller.

5.1.1 Positions and translational velocities

The reference position and velocity of the quadrotor with its actual position and velocity has been shown in Figure 4, Figure 5 and Figure 6 for the axes *x*, *y* and *z* respectively. It has been

Figure 7 (a) Roll angle, (b) pitch angle, (c) yaw angle plot without external disturbances, (d) roll angle, (e) pitch angle and (f) yaw angle plot with external disturbances

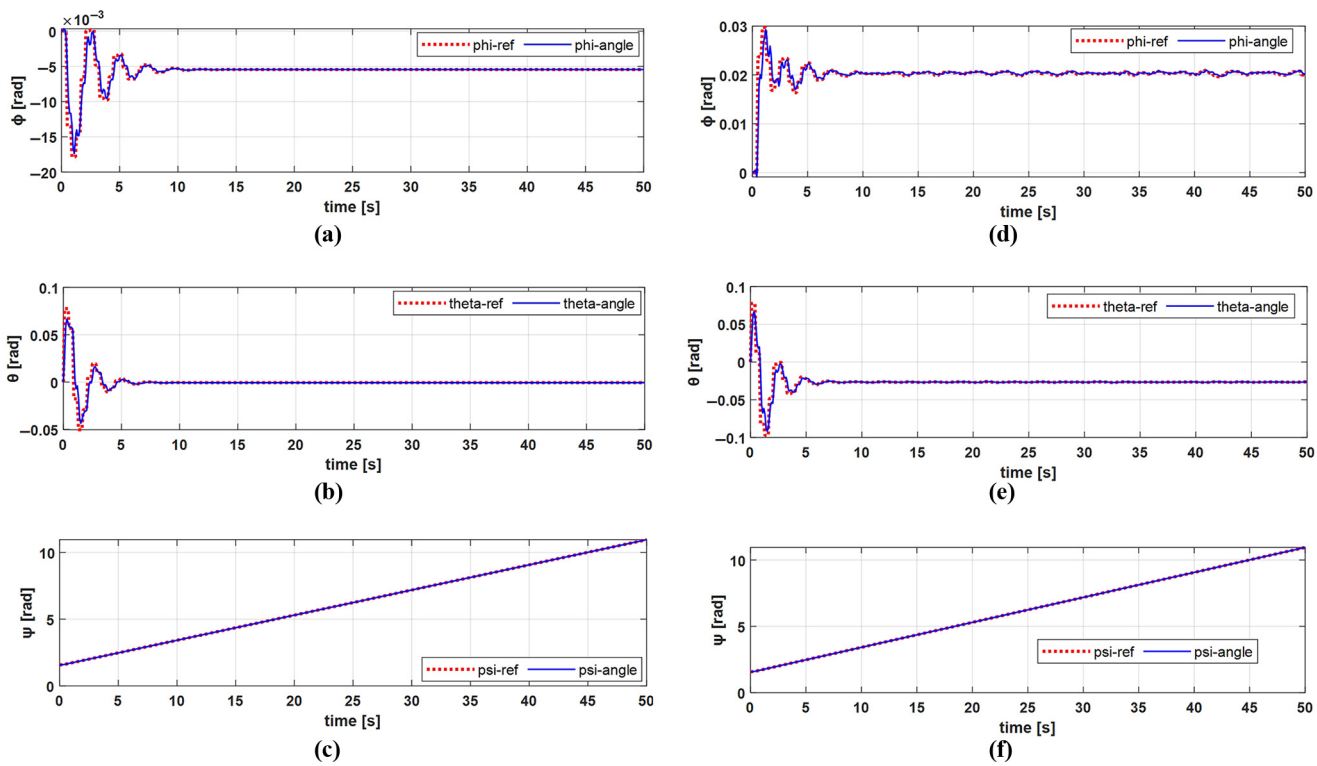

considered in both the cases, one with disturbances and other without disturbance.

5.1.2 Attitude angles

The attitude angles stabilization for the circular path tracking case has been successfully achieved, and their variation with time has been plotted in the Figure 7. The plots in both cases, i.e. with and without external disturbances, will be different because the reference values for roll and pitch angles are provided by position controller. Therefore, in presence of external disturbance, the reference angles are changed little bit.

The variation of the roll angle ϕ and pitch angle θ is very small because of the small angle assumption in the MPC controller design.

5.1.3 Control inputs

The four control inputs, thrust force and three moments across x-, y- and z-axes have been shown in Figure 8.

The plots with solid red line are the inputs in absence of disturbances, and the plots with dotted blue line are control inputs in presence of disturbances.

5.2 Helical trajectory

The controller is again tested for the helical trajectory in the three-dimensional space. The helical trajectory has been generated by the trajectory generator with providing appropriate position for x-, y- and z-direction. The quadrotor trajectory tracking plot has been depicted in Figure 9. The tracking error of the quadrotor has been very small for the given trajectory.

5.2.1 Positions and translational velocities

The reference position and velocity of the quadrotor with its actual position and velocity has been shown in Figure 10, Figure 11 and Figure 12 for the axes x, y and z respectively. It has been considered in both the cases, one with disturbances and other without disturbance. There are some oscillations in the transient period for all the three directions, when the quadrotor takes off the ground and it's almost moving steadily maintaining stability after the flight.

5.2.2 Attitude angles

The attitude angles stabilization for the circular path tracking case has been successfully achieved and their variation with time has been plotted in the Figure 13.

Figure 8 Four control inputs (a) total thrust, (b) moment around x-axis, (c) moment around y-axis, (d) moment around z-axis with and without external disturbances

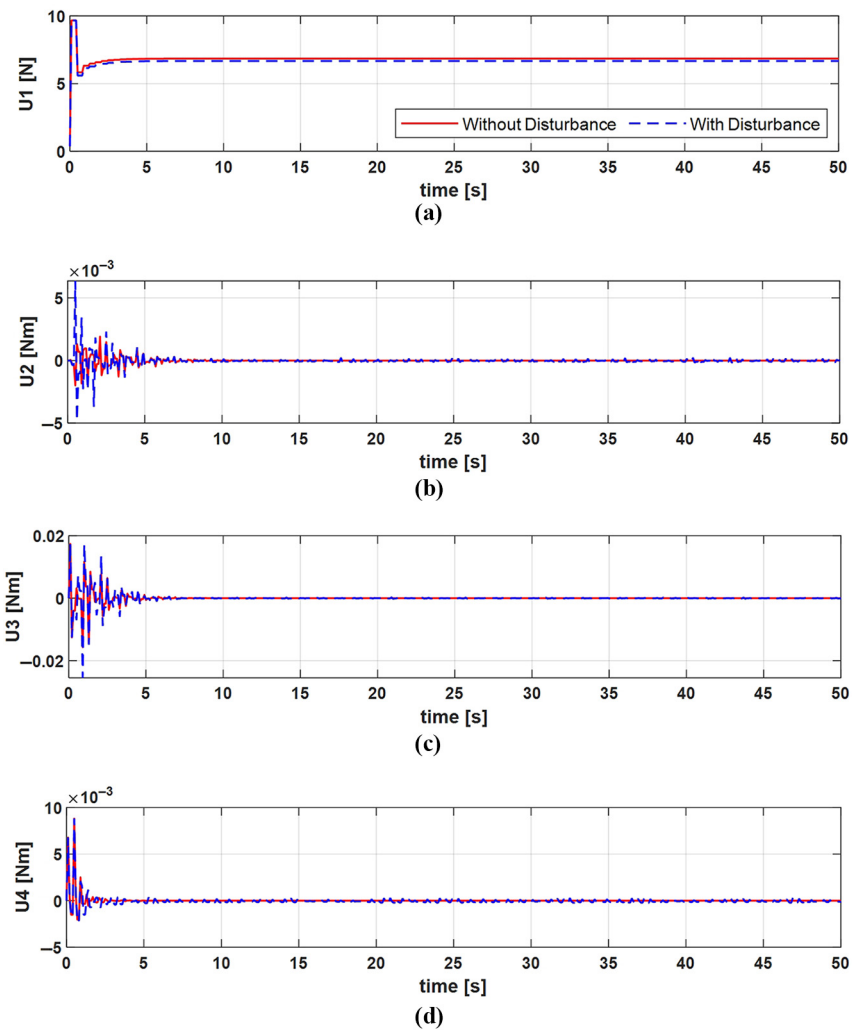

Figure 9 Helical trajectory tracking plot for Quadrotor with and without the external disturbances

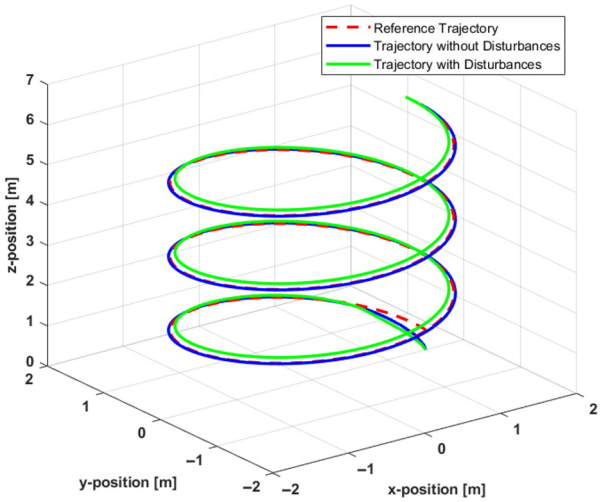

Figure 10 (a) Translational *x*-position (b) *x*-velocity with and without external disturbances

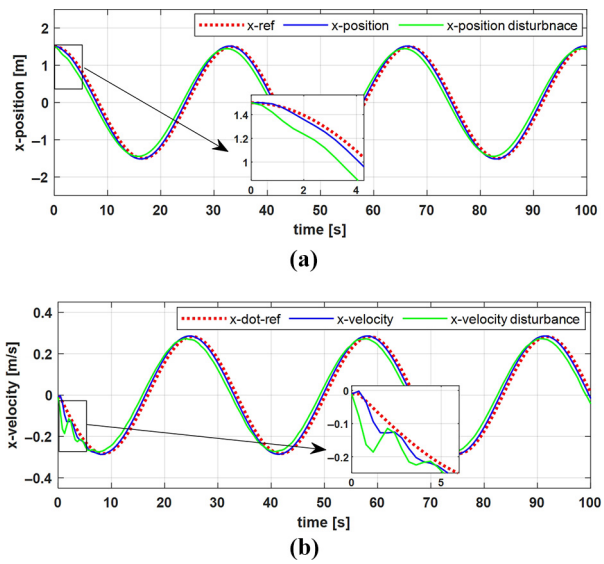

The variation of the roll angle ϕ and pitch angle θ is very small because of the small angle assumption in the MPC controller design.

5.2.3 Control inputs

The four control inputs, thrust force and three moments across *x*-, *y*- and *z*-axes have been shown in Figure 14. The plots with solid red line are shown for the controller performance in absence of the disturbances, and dotted blue lines are for the control action in presence of disturbances.

The controller design for the quadrotor system has been tested for both circular and helical trajectories, and the performance of the controller is found to be very good. The trajectory tracking

Figure 11 (a) Translational *y*-position, (b) *y*-velocity with and without external disturbances

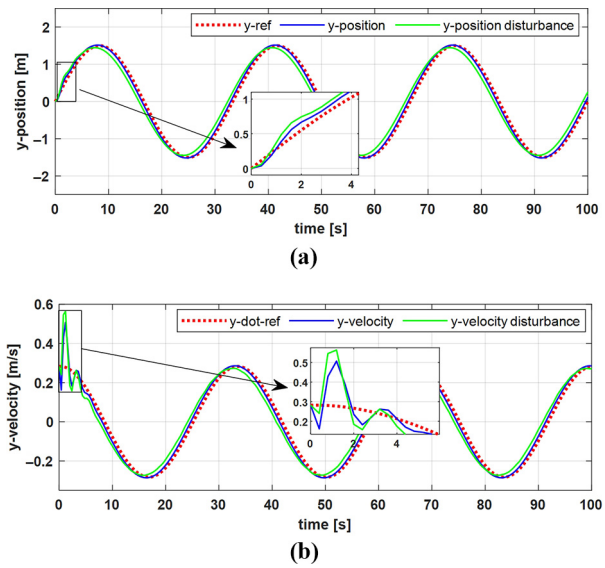

Figure 12 (a) Translational *z*- position, (b) *z*-velocity with and without external disturbances

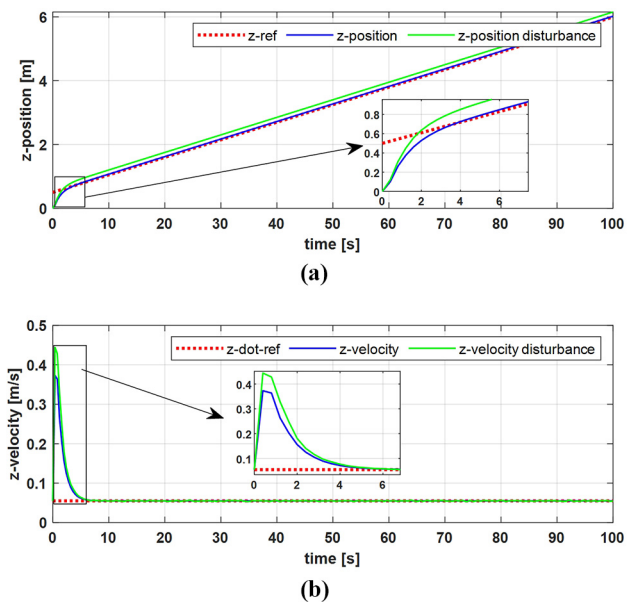

performance of the controllers is very adequate for the given trajectories. The attitude stabilization for the quadrotor has been successfully achieved, and the roll and pitch angle variation are very small as per the small angle approximation. The change in control inputs which is considered as input for the cost function formation is found very advantageous in case of real-time operation of the quadrotor system.

5.3 Comparison of proposed controller

The comparison of the proposed controller has been made based on the root mean square error for tracking of the reference

Figure 13 (a) Roll angle, (b) pitch angle, (c) yaw angle plot without external disturbances, (d) roll angle, (e) pitch angle and (f) yaw angle plot with external disturbances

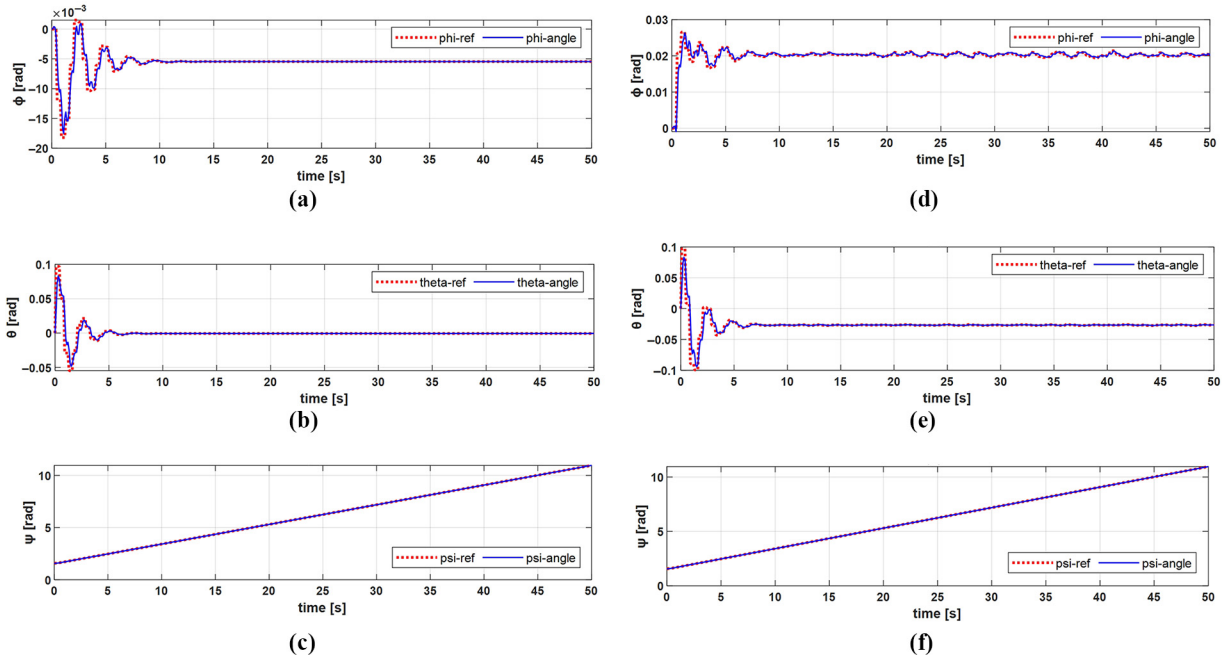

Figure 14 Four control inputs (a) total thrust, (b) moment around *x*-axis, (c) moment around *y*-axis, (d) moment around *z*-axis with and without external disturbances

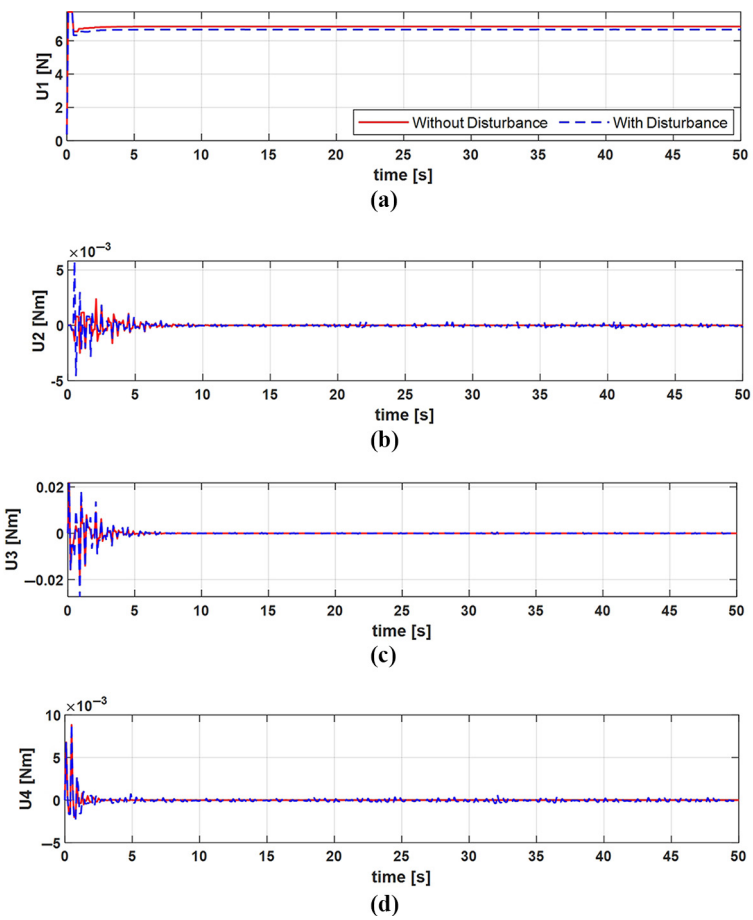

trajectory. The comparison has been made with the LQR–based controller which has been implemented in Martins *et al.* (2019). The root mean square error for the LQR and the proposed technique has been given in the Table 3.

From the Table 3, it is clear that the root mean square errors with the proposed controller is found to be small as compared to the LQR controller. Therefore, the proposed controller shows efficient trajectory tracking ability compared to the LQR. So, it is concluded that the proposed controller shows good performance and trajectory tracking.

5.4 Comments on real-time implementation

There are two factors that are necessary to discuss for the real-time implementation of the proposed control strategy on an actual quadrotor: one is actuator performance and other is computational burden of the controller.

5.4.1 Actuator performance

The control inputs U_1, U_2, U_3 and U_4 obtained from the control action is converted to the motor speeds Ω_1, Ω_2, Ω_3 and Ω_4 with the equations (13) and (14), which are the motor command speed. By analyzing the motor command speed, it was found that the command speeds are physically realizable with the use of electronic speed controller.

5.4.2 Computational burden

The model predictive controller suffers with the problem of high computational burden. But the linear MPC design requires less computational cost as compared to nonlinear MPC, which has been designed in this paper. Still, the computational burden of the linear MPC needs attention owing to continuous optimization of the quadratic cost function. Therefore, a dedicated PC with efficient performance is required for the real-time implementation of the proposed controller. Thus, MPC horizon is so selected to achieve a good compromise between computational burden and the controller performance.

6. Conclusion

In this paper, the QUAV 6-DoF dynamics and its trajectory tracking control for different trajectories have been presented and simulated in MATLAB environment. The feedback linearization and MPC controller for translational and rotational dynamics have been designed and implemented successfully in the presence of external atmospheric disturbances such as wind gust. The combination of both the controllers are used to reduce the computational burden for obtaining the control action. Both the controllers work in coordination with different frequencies of operation to minimize the tracking error of the MPC controller. Both the controllers in combination are tested for circular and helical trajectories. The simulation result shows that the controllers in combination for different trajectories is very efficient in terms of robustness, tracking error and control action. The controller has been designed to work in presence of external disturbances. There are few other challenges as well, such as actuator saturation and noisy measurements that needs to be addressed through state estimator in the control design problem.

Table 3 Comparison of root mean square error values

Technique	x(m)	y(m)	z(m)	ψ(deg)
LQR (Martins *et al.*, 2019)	0.0865	0.0714	0.0556	0.0095
Proposed Controller	0.0648	0.0629	0.0224	0.00016

References

Abdolhosseini, M., Zhang, Y.M. and Rabbath, C.A. (2013), "An efficient model predictive control scheme for an unmanned quadrotor helicopter", *Journal of Intelligent & Robotic Systems*, Vol. 70 Nos 1/4, pp. 27-38.

Alexis, K., Nikolakopoulos, G. and Tzes, A. (2012), "Model predictive quadrotor control: attitude, altitude and position experimental studies", *IET Control Theory & Applications*, Vol. 6 No. 12, pp. 1812-1827.

Bolandi, H., Rezaei, M., Mohsenipour, R., Nemati, H. and Smailzadeh, S.M. (2013), "Attitude control of a quadrotor with optimized PID controller", *Intelligent Control and Automation*, Vol. 4 No. 3, pp. 335-342.

Bouabdallah, S. and Siegwart, R. (2005), "Backstepping and sliding-mode techniques applied to an indoor micro quadrotor", *Proceedings – IEEE International Conference on Robotics and Automation*, pp. 2247-2252.

Cen, R., Jiang, T. and Tang, P. (2021), "Modified Gaussian process regression based adaptive control for quadrotors", *Aerospace Science and Technology*, Vol. 110, p. 106483.

Cervantes, J., Yu, W., Salazar, S. and Chairez, I. (2017), "Takagi-Sugeno dynamic neuro-fuzzy controller of uncertain nonlinear systems", *IEEE Transactions on Fuzzy Systems*, Vol. 25 No. 6, pp. 1601-1615.

Cervantes-Rojas, J.S., Muñoz, F., Chairez, I., González-Hernández, I. and Salazar, S. (2020), "Adaptive tracking control of an unmanned aerial system based on a dynamic neural-fuzzy disturbance estimator", *ISA Transactions*, Vol. 101, pp. 309-326.

Chehadeh, M.S. and Boiko, I. (2019), "Design of rules for in-flight non-parametric tuning of PID controllers for unmanned aerial vehicles", *Journal of the Franklin Institute*, Vol. 356 No. 1, pp. 474-491.

Chen, F., Lei, W., Zhang, K., Tao, G. and Jiang, B. (2016), "A novel nonlinear resilient control for a quadrotor UAV via backstepping control and nonlinear disturbance observer", *Nonlinear Dynamics*, Vol. 85 No. 2, pp. 1281-1295.

Dierks, T. and Jagannathan, S. (2010), "Output feedback control of a quadrotor UAV using neural networks", *IEEE Transactions on Neural Networks*, Vol. 21 No. 1, pp. 50-66.

Efe, M.Ö. (2011), "Neural network assisted computationally simple PIλD μ control of a quadrotor UAV", *IEEE Transactions on Industrial Informatics*, Vol. 7 No. 2, pp. 354-361.

Eltayeb, A., Rahmat, M.F., ad, Basri, M., Eltoum, M. and El-Ferik, S.A.M.A.M. (2020), "An improved design of an adaptive sliding mode controller for chattering attenuation and trajectory tracking of the quadcopter UAV", *IEEE Access*, Vol. 8, pp. 205968-205979.

Freddi, A., Lanzon, A. and Longhi, S. (2011), "A feedback linearization approach to fault tolerance in quadrotor vehicles", *IFAC Proceedings Volumes (IFAC–PapersOnline)*, Vol. 44 No. 1, pp. 5413-5418, doi: 10.3182/20110828-6-IT-1002.02016.

Gai, W., Liu, J., Qu, C. and Zhang, J. (2018), "Trajectory tracking control for a quadrotor UAV via extended state observer", *Systems Science & Control Engineering*, Vol. 6 No. 3, pp. 126-135.

García, O., Santos, O., Romero, H. and Salazar, S. (2016), "On the tracking trajectory using optimal control in a quadrotor helicopter: experimental results", *2015 Workshop on Research, Education and Development of Unmanned Aerial Systems, RED-UAS 2015*, Institute of Electrical and Electronics Engineers, pp. 142-151.

Ghadiri, H., Emami, M. and Khodadadi, H. (2021), "Adaptive super-twisting non-singular terminal sliding mode control for tracking of quadrotor with bounded disturbances", *Aerospace Science and Technology*, Vol. 112, p. 106616.

Guo, M., Su, Y. and Gu, D. (2017), "Mixed H2/H∞ tracking control with constraints for single quadcopter carrying a cable-suspended payload", *IFAC–PapersOnLine*, Vol. 50 No. 1, pp. 4869-4874.

Jia, Z., Yu, J., Mei, Y., Chen, Y., Shen, Y. and Ai, X. (2017), "Integral backstepping sliding mode control for quadrotor helicopter under external uncertain disturbances", *Aerospace Science and Technology*, Vol. 68, pp. 299-307, doi: 10.1016/j.ast.2017.05.022.

Jiang, F., Pourpanah, F. and Hao, Q. (2020), "Design, implementation, and evaluation of a neural-network-based quadcopter UAV system", *IEEE Transactions on Industrial Electronics*, Vol. 67 No. 3, pp. 2076-2085.

Lee, D., Kim, H.J. and Sastry, S. (2009), "Feedback linearization vs. adaptive sliding mode control for a quadrotor helicopter", *International Journal of Control, Automation and Systems*, Vol. 7 No. 3, pp. 419-428.

Liu, H., Zhao, W., Hong, S., Lewis, F.L. and Yu, Y. (2019), "Robust backstepping-based trajectory tracking control for quadrotors with time delays", *IET Control Theory & Applications*, Vol. 13 No. 12, pp. 1945-1954.

Martins, L., Cardeira, C. and Oliveira, P. (2019), "Linear quadratic regulator for trajectory tracking of a quadrotor", *IFAC–PapersOnLine*, Vol. 52 No. 12, pp. 176-181.

Misin, M. and Puig, V. (2020), "LPV MPC control of an autonomous aerial vehicle", *2020 28th Mediterranean Conference on Control and Automation, MED 2020*, pp. 109-114.

Nascimento, R.G., Fricke, K., Viana, F. and A., C. (2020), "Quadcopter control optimization through machine learning", *AIAA Scitech 2020 Forum*, American Institute of Aeronautics and Astronautics Inc, AIAA, Vol. 1, PartF, doi: 10.2514/6.2020-1148.

Oliva-Palomo, F., Muñoz-Vázquez, A.J., Sánchez-Orta, A., Parra-Vega, V., Izaguirre-Espinosa, C. and Castillo, P. (2019), "A fractional nonlinear PI-Structure control for robust attitude tracking of quadrotors", *IEEE Transactions on Aerospace and Electronic Systems*, Vol. 55 No. 6, pp. 2911-2920.

Outeiro, P., Cardeira, C. and Oliveira, P. (2021), "Multiple-model control architecture for a quadrotor with constant unknown mass and inertia", *Mechatronics*, Vol. 73, p. 102455.

Prempain, E. and Postlethwaite, I. (2005), "Static H∞ loop shaping control of a fly-by-wire helicopter", *Automatica, Pergamon*, Vol. 41 No. 9, pp. 1517-1528.

Qiao, J., Liu, Z. and Zhang, Y. (2018), "Gain scheduling based PID control approaches for path tracking and fault tolerant control of a quad-rotor UAV", *International Journal of Mechanical Engineering and Robotics Research*, Vol. 7 No. 4, pp. 401-408.

Sadigh, R.S.M. (2019), "Optimizing PID controller coefficients using fractional order based on intelligent optimization algorithms for quadcopter", *Proceedings of the 6th RSI International Conference on Robotics and Mechatronics, IcRoM 2018*, Institute of Electrical and Electronics Engineers Inc., pp. 146-151.

Salih, A.L., Moghavvemi, M., Mohamed, H.A.F. and Gaeid, K.S. (2010), "Flight PID controller design for a UAV quadrotor", *Scientific Research and Essays, Academic Journals*, Vol. 5 No. 23, pp. 3660-3667.

Santos, O., Romero, H., Salazar, S., García-Pérez, O. and Lozano, R. (2016), "Optimized discrete control law for quadrotor stabilization: experimental results", *Journal of Intelligent & Robotic Systems*, Vol. 84, Nos 1/4, pp. 67-81.

Sol, H., Lee, K. and Hoon, Y. (2021), "Decentralized sampled-data fuzzy controller design for a VTOL UAV", *Journal of the Franklin Institute*, Vol. 358 No. 3, pp. 1888-1914.

Torres, F., Rabhi, A., Lara, D., Romero, G. and Pégard, C. (2016), "Fuzzy state feedback for attitude stabilization of quadrotor", *International Journal of Advanced Robotic Systems*, Vol. 13 No. 1, p. 2.

About the authors

Brajesh Kumar Singh graduated from the M.J.P. Rohilkhand University, Bareilly, Uttar Pradesh, India, with BTech degree in Electrical Engineering in 2013 and MTech (Control and Instrumentation) from Electrical Engineering Department of Madan Mohan Malaviya University of Technology, Gorakhpur. Currently, he is pursuing his PhD at the Electrical Engineering Department, Madan Mohan Malaviya University of Technology Gorakhpur. His research interests include control system, nonlinear control techniques, autonomous aerial vehicle. He is a Student Member of Automatic Control & Dynamic Optimization Society (ACDOS), India. Brajesh Kumar Singh is the corresponding author and can be contacted at: brajeshee@mmmut.ac.in

Awadhesh Kumar is currently working as an Assistant Professor in the Department of Electrical Engineering at Madan Mohan Malaviya University of Technology, Gorakhpur, India. He obtained his PhD in Electrical Engineering from Motilal Nehru National Institute of Technology, Allahabad, India. He did his ME Degree from National Institute of Technical Teachers' Training and Research, Chandigarh, Punjab, India, and BE from Birla Institute of Technology, Mesra, Ranchi, India. His research interests mainly include control systems, model order reduction, applications of optimization and artificial intelligence techniques to control design. He is a Professional Member of Institute of Electrical and Electronics Engineers, Member of Institution of Engineers (India) and Executive Member of ACDOS, India.